RSC Advances

ROYAL SOCIETY OF CHEMISTRY

www.rsc.org/advances

A Bienzyme Immobilized Highly Efficient Niobiumoxide Nanorods Platform for Biomedical Application

Chandan Singh, M.K.Pandey, A.M.Biradar, A. K. Srivastava , Gajjala Sumana*

Biomedical Instrumentation Section, CSIR-National Physical Laboratory,

Dr.K.S.Krishnan Road, New Delhi-110012, India.

Abstract

Electrophoretically deposited niobium oxide nanorods have been utilized to fabricate high performance biosensor for specific cholesterol detection. The orthorhombic structure of Nb_2O_5 platform has resulted in the stable and excellent characteristics of biosensor. This biosensor has been able to detect cholesterol selectively in wide detection range [25-500 mg/dl] with sensitivity of 0.267μA/mgdl^{-1}/cm^2 and re-usability for 10 times, stability for 6 months due to the immobilization of bienzyme on the matrix assisted by intrusion in the Nb_2O_5 nanorods. The low value of Michaelis-Menten constant (0.07 mg/dl) of biosensor indicates higher affinity of bi-enzyme towards cholesterol. The sensor has also been validated with clinical samples.

*Author for correspondence e-mail. sumanagajjala@gmail.com, Phone: +91-11-45609152, Fax: 91-11-45609310.

1 Introduction

Development of miniaturized clinical diagnostic devices has been considered one of the biggest milestones of nanostructured materials.[1,2] Recently, one dimensional (1-D) nanostructured metal oxides have gained much attention in the development of nanosized devices due to its tunable size known as quantum size confinement.[3,4] In particular, metal oxide nanorods are widely used in the development of electrochemical biosensor due to channeling effect leading to improved electron transfer properties.[5-8] The nanorods offer higher area-scaffolds for functionalization of bio-molecules and can act as mediator which introduce a conduction channel for electron transport from redox enzyme to current collector.[9] Many researchers have explored 1-D metal oxides of nickel, zinc, iron, niobium etc. for biosensor development.[10,11] Thus, nanorods having conducing electron transfer and catalytic properties could be an efficient platform for clinical diagnostic applications.

Niobium oxide (Nb_2O_5) is known to be n-type semiconducting material and has a significant potential for various applications in electrochromism, gas sensing and field emission displays etc.[12-14] Among various polymorphs of niobium oxide, orthorhombic form (T-Nb_2O_5)is thermodynamically stable phase with high catalytic and electrochemical activity, biocompatibility and surface reactivity properties due to its intrinsic defects.[15,16] In addition, high crystalline structure of Nb_2O_5 could be considered to improve charge transfer properties towards biosensing applications. In this context, the large amount of oxygen vacancies present in T-Nb_2O_5 may help in the proper immobilization of the biomolecules. In the fabrication of electrochemical biosensor, electrical contacting of redox-enzymes with electrodes is an important step. In this regard, enzymes lack direct electrical communication

with electrodes due to the fact that the active centers of enzymes are surrounded by considerably thick insulating protein shells leading to block the enzyme active centers.[17]

Nb_2O_5 is known to overcome this problem due to its intrinsic electrochemical properties and can promote direct electron transfer of redox proteins even when the active centers are distant from the electrode surface.[18] In addition, the catalytic properties of nanoparticles may perhaps influence and enhance the electrochemical sensing behaviour. You et al. have reported the role of catalytic platinum nanoparticles in a highly sensitive H_2O_2 sensor, while Xu et al. have described the significance of catalytic properties of copper oxide nanoparticles in enhanced current for electrochemical detection of amikacin.[19, 20] Choi et al. have developed cost effective and reliable device based on nanoporous niobium oxide for label-free detection of DNA hybridization events.[21] Xu et al. have used ordered mesoporous Nb_2O_5 as a supporting material for cytocrome-c immobilization.[18] Lee et al. have fabricated a highly sensitive immunosensor based on nanoporous Nb_2O_5 electrode.[22] Thus, intrinsic electrochemical and catalytic properties of Nb_2O_5 with combination of excellent properties of 1D nanomaterials provides considerable scope to construct electrochemical biosensor with improved sensing parameters.

To the best of our knowledge, we are reporting the fabrication of biosensor based on niobium oxide nanorods for cholesterol biosensing for the first time. Fabrication of niobium oxide nanorods based cholesterol biosensor for clinical diagnostics may provide advantages relating to the open structures in the biocompatible rods that may act as host for enzyme entrapment and stable attachment of the bioanalyte. Proper trapping of the enzyme in the space available onto the Nb_2O_5NR film gives increased stabilization which may probably enhance the stability and sensitivity of the fabricated biosensor.

Therefore, in the present manuscript, we report the results relating to the fabrication of electrophoretically deposited Nb_2O_5 nanorods based biosensor that has been used to directly detect total cholesterol level in human serum samples. Physiological level of cholesterol in healthy adults should be less than 200 mg/dl. High blood cholesterol level (>240 mg/dl) is associated with atherosclerosis and causes coronary heart diseases and heart attack while the low blood cholesterol (<80 mg/dl) is linked with hyperthyroidism, cerebral and thrombosis.[23, 24]

2. Materials and methods

2.1 Reagents

Cholestrol oxidase (ChOx), cholesterol esterase (ChEt), cholesterol oleate, cetyl trimethyl ammonium bromide (CTAB) are procured from Sigma-Aldrich (USA). Anhydrous niobium (V) chloride is procured from Alfa Aesar (UK). Indium tin oxide (ITO) coated glass substrates have been obtained from Blazers, UK.

2.2 Fabrication of Nb_2O_5 nanorods based film

Niobium penta-oxide nanorods (Nb_2O_5NR) are prepared by sol-gel method using CTAB as a surfactant. 5 gm of niobium chloride ($NbCl_5$) is dissolved in 10 ml of ethanol, and a clear yellow solution is obtained after stirring at room temperature. 2ml of CTAB (0.2 M) surfactant is added drop wise in the above prepared solution followed by the ammonia solution at pH 12.0 to get white precipitate of ($Nb_2O_5{\cdot}nH_2O$). The obtained ($Nb_2O_5{\cdot}nH_2O$) precipitate is washed for several times with initially deionized water followed by ethyl alcohol to reduce agglomeration and remove the soluble impurities. The separation of liquid and solid phase is made by centrifugation at 4000 rpm for 5min and the resultant ($Nb_2O_5{\cdot}nH_2O$) powder is dried at 80^{o}C for 12h. The existence of different polymorphs of niobium oxide depends on the calcination temperature and follows Eq. (1).[25]

$$(Nb_2O_5.nH_2O)_{(amorphous)} \xrightarrow{300-500^{\circ}C} TT-Nb_2O_{5(pseudo-hexagonal)} \xrightarrow{500-800^{\circ}C} T-Nb_2O_{5(orthorombic)} \quad (1)$$

The ($Nb_2O_5{\cdot}nH_2O$) was calcinated at 750°C for 6h to form T-Nb_2O_5 nanorods, which was further confirmed using X-ray diffraction studies. Further, Nb_2O_5 nanorods were deposited on ITO coated glass substrates using electrophoretic deposition (EPD). The EPD of niobium oxide nanorods (Nb_2O_5NR) was carried out by applying constant anodic potential of 45 V for 1min in the colloidal suspension of Nb_2O_5 nanorods in acetonitrile.

2.3 Immobilization of ChEt-ChOx:

For immobilization, 10µl of prepared mixture of ChEt and ChOx (ratio 1:1, 1.0 mg/ml, in phosphate buffer, 50 mM, pH 7.0) was uniformly spread and kept in a humid chamber condition for 6 h.[Fig.(1)]

3. Characterization

The Nb_2O_5NR film has been characterized using X-ray diffractometer (XRD, Model Max-2200 diffractometer, Rigaku). Scanning electron microscopy (SEM, LEO 440), Fourier-transform infrared spectroscopy (FT-IR, Model 2000, Perkin-Elmer) and high resolution-transmission electron microscopy (HR-TEM, JEOL JEM-2000 EX) to investigate the structure and morphology of Nb_2O_5NR/ITO film and ChEt-ChOx/Nb_2O_5NR/ITO film. Elecctrochemical characterization has been carried out using Autolab Potentiostat/Galvanostat (Eco Chemie, AUT-84275) in phosphate buffer (50 mM, pH7.0, 0.9% NaCl) containing (5mM) $[Fe(CN)_6]^{3-/4-}$ as a redox species using platinum as counter electrode and Ag/AgCl as reference electrode.

4. Results and discussion

4.1 X-ray diffraction (XRD) studies

The XRD pattern of Nb_2O_5NR reveals the orthorhombic structure of Nb_2O_5. The different diffraction planes (001), (180), (200), (181), (201), (002) have been observed at 2θ positions 22.5°, 28.3°, 28.9°, 36.4° 36.9°, 45.9° respectively, as shown in spectrum Fig.[2(A)]. The results indicate that orthorhombic structure of Nb_2O_5 is highly crystalline in nature. The maximum intensities have been observed at (001) and (180) planes. The intensity ratio of (001) and (180) planes is calculated as 1.06 which is higher than that of bulk Nb_2O_5 [JCPDS 27-1003] indicating that preferential nanorods growth along the (001) directions. The average crystallite size for (001) and (180) planes are calculated as 25 nm and 13 nm using Debye-Schereer equation.[26]

4.2 Fourier-transform infrared spectroscopy (FT-IR) studies

Figure [2(A)] shows FTIR spectrum of electrophoretically deposited Nb_2O_5NR/ITO film (curve a), 1:1 mixture of cholesterol oxidase and cholesterol esterase in KBr (curve b) and ChEt-ChOx/Nb_2O_5NR/ITO bioelectrode film (curve c). In curve (a), FTIR spectrum shows stretching bands in the region from 650 to 900 cm^{-1} corresponding to Nb-O stretching and Nb-O-Nb bridging. [27] FTIR spectrum of ChEt-ChOx [curve b] indicate the peaks at 1550 and 1655 cm^{-1} due to amide bonds present in the enzymes. The peak at 1655 cm^{-1} is due to C=O stretching (amide I band), whereas peak at 1550 cm^{-1} originates from the N-H bending (amide II band). The peaks seen at 1400 and 1100 cm^{-1} correspond to the asymmetric and symmetric bending vibrations of C-H groups. The broad peaks in the range of 3200-3500 cm^{-1} are due to the N-H stretching.[28] In curve (c), FTIR spectrum of ChEt-ChOx/Nb_2O_5NR/ITO show all the characteristic peaks of the bienzyme which are clearly visible, indicating the immobilization of enzyme mixture onto the Nb_2O_5NR/ITO film.[29]

4.3 Scanning electron microscopy (SEM) studies

The SEM [Fig. 3(A)] indicates the nanorod morphology of Nb_2O_5 aggregated on ITO surface due to electrophoretic deposition under high potential. It has been seen that these nanorods orient themselves to form films. Further, there are significant open structures in the Nb_2O_5NR film which may act as host for absorption and further sensing of guest enzymes. After immobilization of ChEt-ChOx, the SEM investigations indicate the uniform bienzyme coating on Nb_2O_5 film surface because of its three-dimensional structure [Fig.3 (B)]. Again, the image of ChEt-ChOx/Nb_2O_5NR/ITO film exhibits homogeneous distribution of Nb_2O_5 nanorods with bienzyme which is relatively smooth and crack free. Further, the energy dispersive X-ray spectroscopy (EDX) analysis has been carried out for the elemental analysis of fabricated films. The peaks corresponding to niobium and oxygen have been observed indicating the deposition of Nb_2O_5 onto ITO substrate [Fig. 3 (C)]. The presence of other elements (Sn, Si and In) is attributed to the surface of glassy ITO electrode. The EDX spectrum of ChEt-ChOx/Nb_2O_5NR/ITO film shows additional peaks phosphorous and sodium due to bienzyme interaction with nanorods indicating the immobilization [Fig. 3 (D)].

4.4 High resolution-transmission electron microscopy (HRTEM) studies

The HRTEM studies have been conducted to investigate shape and size of the synthesized Nb_2O_5 nanorods dispersed in acetonitrile. The image shows overview of randomly oriented Nb_2O_5 nanorods [Fig. 4(A)]. It has been observed that the Nb_2O_5 nanorods having low aspect ratio (~3) with diameter 75 nm and average length of 200 nm indicate that the nanorods morphology. The individual Nb_2O_5 nanorod is shown in inset and the end of nanorods appear as conical tip. The atomic scale image shows the Nb_2O_5 nanorods are highly crystalline in nature [Fig.4 (B)]. Clearly visualize lattice fringes of the planes (001) and (180) are overlapped. The lattice spacing has been estimated as 0.39 nm and 0.32 nm for (hkl) value of (001) and (180) respectively. The intensity of the (001) plane is higher compared to that of

(180) plane indicating the preferred crystallization of nanorods are along the (001) direction. These results are in strong agreement with the XRD studies.

4.5 Cyclic voltammetric characterization studies

The cyclic voltammetric (CV) studies of Nb_2O_5NR/ITO electrode and ChEt-ChOx/ Nb_2O_5NR/ITO bioelectrode have been investigated in PBS containing $[Fe(CN)_6]^{3-/4-}$ in the range of -0.5 V to +0.7 V at the scan rate of 50 mVs^{-1} [Fig. 5 (A)].The results of CV studies indicate that magnitude of the current (0.79 mA, curve b) of Nb_2O_5NR/ITO electrode is enhanced as compared to that of bare ITO (0.72 mA, curve a). The presence of Nb_2O_5NR onto ITO surface may help to mediate redox species $Fe^{2+/3+}$ towards electrode from bulk solution that facilitates electrochemical current. Further, improved orientation of Nb_2O_5 nanorods onto the ITO surface can also play an important role in the enhancement of current. Intrinsic electrochemical and catalytic properties of Nb_2O_5 may also be responsible for enhanced current.[30, 31] In addition, it has been observed that the peak-to-peak potential of Nb_2O_5NR/ITO electrode shifts towards the higher side compared to ITO electrode. After the immobilization of bienzyme (ChEt-ChOx) onto Nb_2O_5NR/ITO electrode, the magnitude of current is found to decrease (curve c), due to the insulating nature of bienzyme which obstructs the acceleration of electron transfer between enzyme active sites and the electrode.

The CV studies have been performed for the ChEt-ChOx/Nb_2O_5NR/ITO bioelectrodes as a function of scan rate ranging from 10-100 mV/S [Fig. 5(B)].Magnitude of both anodic and cathodic currents are increased linearly and corresponding peaks are shifted towards the positive and negative potential respectively, with varying scan rate indicating uniform facile charge transfer [Eq. (2) and (3)]. The proportional increase in the anodic and cathodic peak potential as a function of scan rate obeys [Eq. (4) and (5)] indicating the electrochemical reaction is diffusion controlled [Fig.5 (B), Inset (i) & (ii)].

$$Ia\ [A] = -7.40 \times 10^{-5}\ [A] + 7.23 \times 10^{-5}\ [A^2 s/mV]^{1/2} \times [scan\ rate\ (mV/s)]^{1/2} \quad (2)$$

$$Ic\ [A] = -2.0 \times 10^{-4}\ [A] - 4.2 \times 10^{-5}\ [A^2 s/mV]^{1/2} \times \left[scan\ rate\ \left(\frac{mV}{s}\right)\right]^{1/2} \quad (3)$$

$$Vap = 0.27\ (V) + 3.1 \times 10^{-3}(s) * \left[scan\ rate\ \left(\frac{mV}{s}\right)\right] \quad (4)$$

$$Vcp = -0.13\ (V) - 1.63 \times 10^{-3}\ (s) * \left[scan\ rate\ \left(\frac{mV}{s}\right)\right] \quad (5)$$

Charge associated with the adsorption/desorption of an adsorbate gives an indication of the number of surface catalyst atoms present in the electrode. The electrical charge (Q) is defined as the integral of cell current (I) with respect to time (t) $[Q = \int I\, dt]$. The adsorption charge associated with a known adsorbate on the electrode surface (Q_m) and the charge associated with monolayer coverage of the said adsorbate (Q_{ad}), can be related to the electrochemical surface area, $A_{ec}(cm^2) = Q_{ad}/Q_m$. The concentration of electroactive bienzyme associated with the Nb_2O_5NR surface was determined by integrating the anodic peak according the [Eq. (6)]

$$\Gamma = \frac{Q}{nFA_{EC}} \quad (6)$$

where Γ is number of mol/cm^2, Q is the charge obtained by integrating the anodic peak, n is number of electrons involved in the reaction (1) and F is Faraday's constant. It has been found that the surface concentration of the ChEt-ChOx/Nb_2O_5NR/ITO is 7.6×10^{-8} mol/cm^2. The diffusion coefficient (or diffusivity) of electrolyte containing $Fe^{3+/2+}$ ions from CV response with respect to scan rate has been estimated using the [Eq. (7)].

$$i_p/v^{1/2} = Slope = (269{,}000)n^{3/2}AD^{1/2}C \quad (7)$$

where i_p = redox peak current (A), n = number of electrons transferred in the redox event (1), A= electrochemical electrode area (cm^2), D = diffusion coefficient (cm^2/s), C = concentration of redox species (mol/cm^3), ν = scan rate (mV/s)]. The higher diffusivity 1.44×10^{-13}cm^3/s of ions for ChEt-ChOx/Nb_2O_5NR/ITO bioelectrode may be responsible for fast response times.

4.6 Electrochemical response studies

Electrochemical response studies of ChEt-ChOx/Nb_2O_5NR/ITO bioelectrode have been conducted as a function of cholesterol oleate concentration (25-500 mg/dl) [Fig. 5(C)]. It has been observed that current signal increases with increasing concentration of cholesterol oleate in the range of 25-500mg/dl. The electron generation mechanism can easily be explained using biochemical reaction. Initially, the cholesterol oleate are hydrolyzed in presence of ChEt and produced the cholesterol (or 3β-hydroxysteroids) and fatty acid. Since ChOx is a favin adenine dinucleotide (FAD) contacting enzymes that catalyses the oxidation and the isomerization of 3β-hydroxysteroids resulted in final product of Δ^4-3-ketosteroid and hydrogen peroxide and at an applied potential of 0.4V, H_2O_2 produces water and electrons.[32]These electrons are directly accepted by the Nb_2O_5NR and intrinsic electrochemical and catalytic properties that provides a rapid platform for the transport of electrons leading to enhanced sensitivity and response time.

The sensitivity of ChEt-ChOx/Nb_2O_5NR/ITO bioelectrode is found to be 0.267μA/mgdl^{-1}/cm^2 with linear regression coefficient (R^2) 0.998. In addition, the intrinsic electrochemical and catalytic properties of Nb_2O_5 may contribute significantly in enhanced sensitivity of ChEt-ChOx/Nb_2O_5NR/ITO.[17,18] The response time of ChEt-ChOx/Nb_2O_5NR/ITO biosensor found to be as less than 10 s [data not shown]. The fast response may be due to nanorods formation of Nb_2O_5 that enforce the charge separation and thereby ensure that faster transport results in a longer diffusion length. The detection limit is found to be 39.0 mg/dl. Further, the Michaelis-Menten constant (K_m) for this bioelectrode is calculated as 0.002 mM (0.07 mg/dl) using Hanes–Woolf plot indicating excellent affinity towards cholesterol [Fig. 5(C), inset (ii)]. The performance of the biosensor for cholesterol detection has been compared with the reported literature as shown in Table(1) and the comparison clearly indicates the lower K_m in the present work indicating the better enzyme-analyte affinity using niobium oxide nanorods [Table (1)].

4.7 Clinical sample analysis

The response studies of the ChEt-ChOx/Nb_2O_5NR/ITO bioelectrode have been carried out in presence of clinical sample with varying cholesterol concentrations. Serum samples of patients along with clinical data of cholesterol levels have been collected from North Delhi Pathology Clinic, New Delhi (India). In comparison to the standard cholesterol concentration, it has been observed that the ChEt-ChOx/Nb_2O_5NR/ITO bioelectrode shows minute difference of 4.3-8.9% during cholesterol detection in clinical serum samples [Fig. 5(D)]. The concentration versus current response studies with clinical patient samples indicates the nearly linear response indicating a great potential towards the development of point of care diagnostics. Thus, these results indicate that this novel biosensor has potential to detect cholesterol directly in human serum sample.

4.8 Stability and Reproducibility studies

The storage stability of bioelectrode has been monitored by measuring the cholesterol concentration at regular time intervals. It has been found that the bioelectrode retain about 90% of the activity even after 6 months when stored in refrigerated conditions [Fig. 6]. The proposed ChEt-ChOx/Nb_2O_5NR/ITO bioelectrode shows good reproducibility for different working electrodes fabricated trough similar procedure with cholesterol concentration 100 mg/dl. For reproducibility test, we have considered eight different bioelectrodes with constant sensor surface area and it has been found that this bioelectrodes shows negligible variation in the current response as evidenced by the relative standard deviation (RSD) of 0.80% (mean value = 539.5μA). The low RSD of this fabricated ChEt-ChOx/Nb_2O_5NR/ITO biosensor indicates good precision [Fig.7].

4.9 Selectivity studies

The selectivity of the ChEt-ChOx/Nb_2O_5NR/ITO bioelectrode for specific cholesterol detection is investigated by measuring the response characteristics of the mixture of

cholesterol of (200 mg/dl) and interferents such as glucose, lactic acid, ascorbic acid, urea, uric acid and paracetamol in 1:1 ratio. The concentration of these interferants was taken as 10 times higher than the concentration of the cholesterol. The change in the response current was found to be negligible, which has been found to be in the range 0.44 to 2.2 % in presence of potential interferrents of concentration 10 times more than that of cholesterol. Our results indicate that there was almost negligible change in the current response in presence of interferents indicating that the bioelectrodes is highly specific for cholesterol detection [Fig. 8]. The bioelectrode has also been found to be reusable more than for 10 times. The performance of the biosensor has been compared with the reported literature and the comparison with the reported literature indicates that the sensor shows the improved stability and is attributed to the stable immobilization of the bienzyme onto the niobium oxide nanorods [Table 1].

5. Conclusions

We have demonstrated the fabrication of a biosensor based on electrophoretically deposited niobium oxide nanorods for the detection of total cholesterol directly from human serum sample. It has been observed that these nanorods have potential to attach bienzyme directly for target analyte detection from serum sample. The biosensor has been found to be sensitive in a wide detection range (25-500 mg/dl) with the stability of more than 6 months. This approach may find applications in the sensitive detection of other analytes such as glucose, urea, uric acid, paracetamol and has implications in the development of point of care diagnostics.

6. Acknowledgements

We are thankful to Prof. R.C.Budhani, Director, CSIR- NPL, India for providing facilities to carry out this work. We thank Prof. B. D. Malhotra, Delhi Technological University and Md.

Azahar Ali, CSIR-NPL for useful discussions. We thank Dr. Rakesh Sharma, North Delhi Pathology Clinic for providing the clinical patient samples and standard data of cholesterol in patients. Financial support received from Department of Science and Technology (GAP-081132) is gratefully acknowledged.

References:

1 P.K. Jain, X. Huang, H.Ivan, M.El-Sayed and A. El-Sayed, *Acc. Chem. Res*.,2008, 41, 1578.

2 D.A. Giljohann and C.A. Mirkin, *Nature,* 2009, 462, 461.

3 Y.Xia, P.Yung, Y Sun, Y.Wu, B.Mayers, B.Gates, Y.Yin, F.Kim and H.Yan*, Adv. Mater*., 2003, 15, 353.

4 Z. L.Wang, *Adv Mater*.,2000,12, 1295.

5 J. Hu, T.W. Odom and C.M. Lieber, *Acc. Chem. Res*., 1999, 20, 435.

6 H. Wang, Z. Lu, D.Qian, Y. Liand and W.Zhang, *Nanotechnology*, 2007, 18, 15616.

7 G. Wang, D. Chen, H. Zhang, J. Z. Zhang, and J. Li, J. Phys. Chem.C.,2008, 112, 8850.

8 G.Gruner, *Anal. Bioanal. Chem*., 2006, 384, 322.

9 J.Liu,Y.Li,X.Huang and Z.Zhu*, Nanoscale Res Lett*.,2010,5,1177.

10 Md.A.Ali, P.R.Solanki, M.K.Patel, H.Dhayani, V.V.Agrawal, R.John and B.D. Malhotra, *Nanoscale*, 2013, 5, 2883.

11 F.Zhang, X.Wang, S. Ai, Z.Sun, Q. Wan, Z. Zhu, Y.Xian, L.Jin and K.Yamamoto. *Anal Chim Acta.*, 2004, 2, 519.

12 Y.D. Wang, L.F. Yang, Z.L. Zhou, Y.F. Li and X.H. Wu, *Mater Lett*., 2001, 49, 277.

13 P.Carniti , A. Gervasini and M. Marzo, *J Phys Chem C*.,2008, 112,14064 .

14 S.H. Mujawar, A.I. Inamdar, S.B. Patil and P.S. Patil, *Solid State Ionics*, 2006, 177, 3333.

15 Y. Zhao, X. Zhou, L. Ye and S. C. E.Tsang, *Nano Reviews*, 2012, 3,17631.

16 Y.Zhou, Z .Qiu, M. Lu, A .Zhang, Q. Ma, *J Lumin.*, 2008, 128, 1369.

17 X. Luo, A.Morrin, A.J. Killard and M. R. Smyth, *Electroanalysis*,2006, 18, 319.

18 X.Xu, B.Tian, J.Kong,S.Zhang,B.Liu and D.Zhao, Adv. Mater.,2003, 15,1932.

19 T. You, O. Niwa, M. Tomita and S. Hirono, *Anal. Chem*.,2003, 75, 2080.

20 J. Z. Xu, J. J. Zhu, H. Wang and H. Y. Chen, *Anal. Lett.,* 2003, 36, 2723.

21 J. Choi J.H.Lim, S. Rho, D.Jahng, J. Lee and K. Kim, *Talanta*, 2008, 74,1056.

22 C.S. Lee, D.Kwon, J.E. Yoo, B.G. Lee, J. Choi, B.H. Chung. *Sensors*, 2010,10,5160.

23 L.Pollegioni, L.Piubelli and G.Molla, *The FEBS Journal*, 2009, 276, 6857.

24 L.Puglielli, A.L. Friedlich, K.D.R. Setchell, S. Nagano, C. Opazo, R. A. Cherny, K.J. Barnham, J.D.Wade, S.Melov and D.M.Kovacs, *J Clin Inves*., 2005,115, 2556.

25 R. Brayner and F. B.Verduraz, *Phys. Chem. Chem. Phys*., 2003, 5, 1457.

26 U.Holzwarth and N.Gibson, *Nat Nanotechnol*., 2011, 6, 534.

27 H. Y. Y. Ko, M. Mizuhata, A. Kajinami and S. Deki, *J. Mater. Chem*., 2002, 12, 1495.

28 P. Solanki, A. Kaushik, A. Ansari and B. D. Malhotra, *Appl. Phys.Lett*.,2009, 94, 14390.

29 A. A. Ansari, A. Kaushik, P. R. Solanki and B. D. Malhotra, *Electrochem. Commun*., 2008,10, 1246.

30 J. Z. Xu, J. J. Zhu, H. Wang and H. Y. Chen, *Anal. Lett* ., 2003,36, 2723.

31 J. Choi J.H.Lim, S. Rho, D.Jahng, J. Lee and K. Kim, *Talanta*, 2008, 74,1056.

32 S. K. Arya, M. Datta and B. D. Malhotra, *Biosens. Bioelectron*., 2008, 23, 1083.

33 G.K. Kouassi, J. Irudayaraj and G. McCarty. *J. Nanotechnol*.,2005, 3, 1477.

34 S.P. Singh, S.K. Arya, P. Pandey, B.D. Malhotra, S. Saha, K. Sreenivas and V. Gupta, *Appl. Phys. Lett*.,2007, 91, 63901.

35 J. Singh, P. Kalita, M. K. Singh and B. D. Malhotra, *Appl. Phys. Lett*., 2011, 98, 123702.

36 A. Salimi, R. Hallaj and S. Soltanian, *Electroanalysis*, 2009, 21, 2693.

37 J. Singh, A. Roychoudhary, M. Srivastava, P.R. Solanki, D. W. Lee, S. H. Lee and B.D.Malhotra, *Nanoscale*, 2014,6, 1195.

Figure Captions:

FIG.1. Schematic representation of the fabrication of Nb_2O_5 nanorods based biosensor for clinical diagnostic of cholesterol.

FIG.2. (A) XRD pattern of Nb_2O_5 nanorods. **(B)** FTIR spectra of Nb_2O_5NR/ITO film (curve a), FTIR spectra of enzyme ChEt-ChOx in KBr (curve b). FTIR spectra of ChEt-ChOx/ Nb_2O_5NR/ITO bioelectrode (curve c).

FIG.3 (A) Scanning electron microscopy images of Nb_2O_5NR/ITO film. **(B)** Scanning electron microscopy image of ChEt-ChOx/Nb_2O_5NR/ITO bioelectrode. **(C)** Energy Dispersive X-Ray spectrum of Nb_2O_5NR/ITO film. **(D)** Energy Dispersive X-Ray spectrum of ChEt-ChOx/Nb_2O_5NR/ITO bioelectrodes.

FIG.4 (A) Transmission electron microscopy image of Nb_2O_5 nanorods. **(B)** High resolution transmission electron microscopy image of Nb_2O_5 nanorods.

FIG.5 (A) CV studies of bare ITO, Nb_2O_5NR/ITO and ChEt-ChOx/Nb_2O_5NR/ITO bioelectrode. **(B)** Cyclic voltammetric response studies of ChEt-ChOx/Nb_2O_5NR/ITO as a function of scan rate. **(C)** Electrochemical response of ChEt-ChOx/Nb_2O_5NR/ITO bioelectrode at different concentrations (25-500 mg/dl) of cholesterol oleate in phosphate buffer. Inset (i) Linearity between current and concentration. Inset (ii) Hanes-Woolf plot between substrate concentration and concentration/current. **(D)** Electrochemical response of ChEt-ChOx/Nb_2O_5NR/ITO bioelectrode at different concentrations available clinical samples. Inset (i) Linearity between current and clinical sample concentrations.

FIG.6 Stability studies of ChEt-ChOx/Nb_2O_5NR/ITO bioelectrodes.

FIG.7 Reproducibility studies of ChEt-ChOx/Nb_2O_5NR/ITO bioelectrode.

FIG.8 Specificity studies of ChEt-ChOx/Nb_2O_5NR/ITO bioelectrode in presence of different bioanalytes.

TABLE.1: Comparison table on performance characteristics of metal oxide based cholesterol biosensor.

Figures and Table

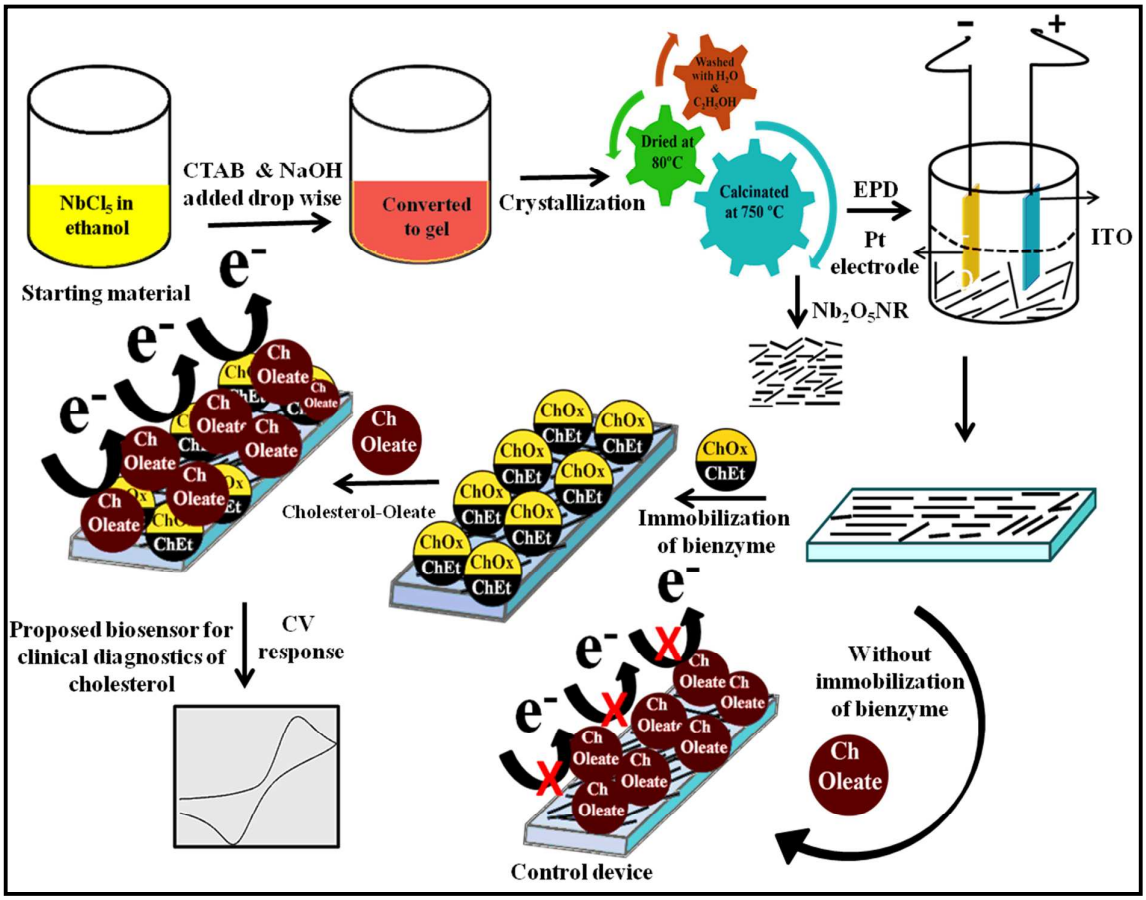

FIG.1

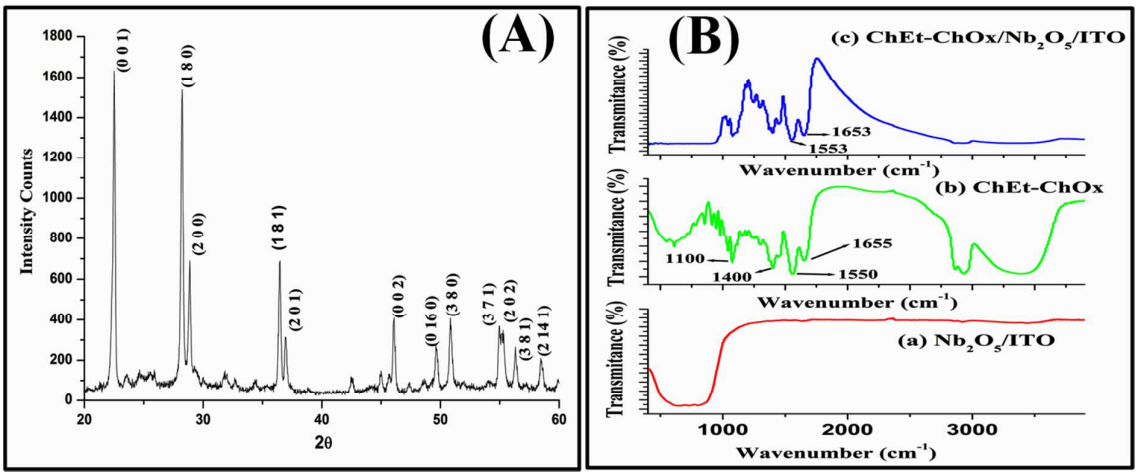

FIG.2

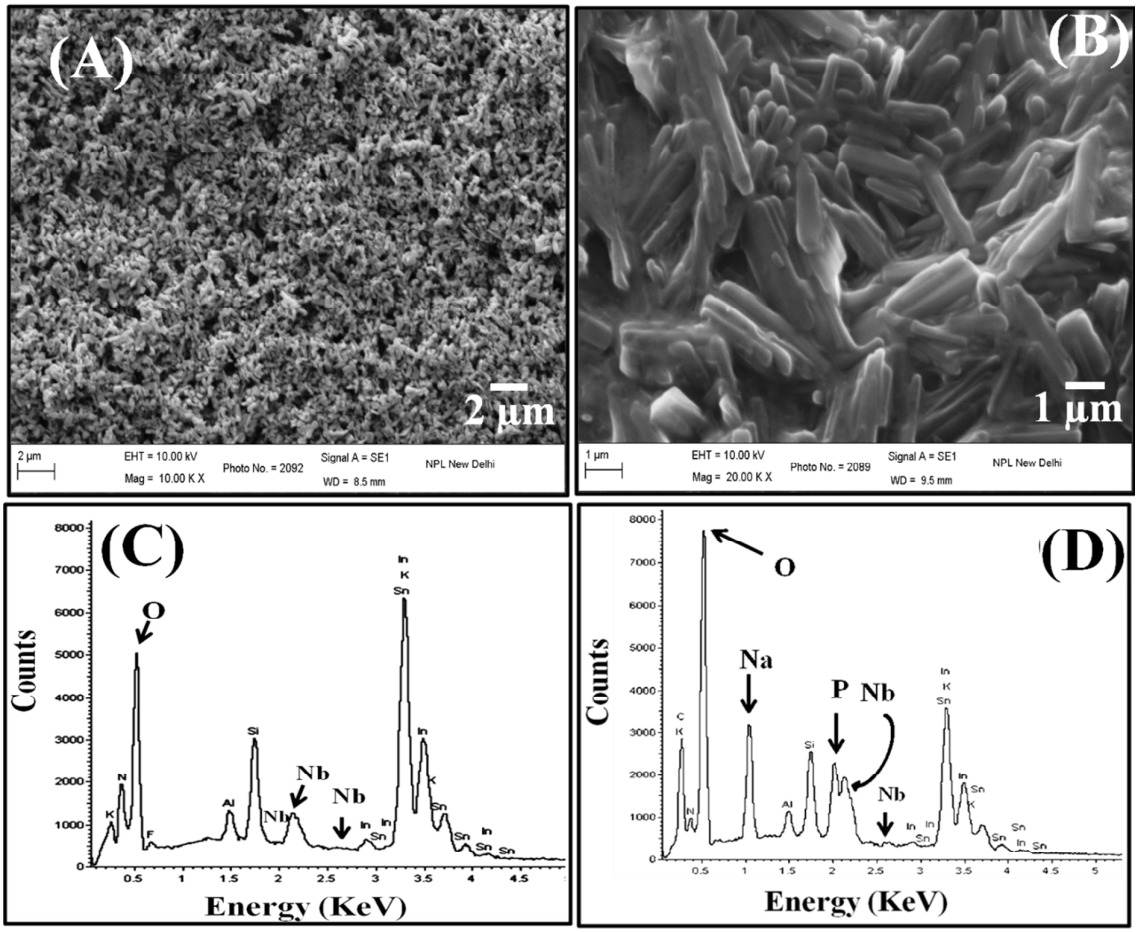

FIG.3

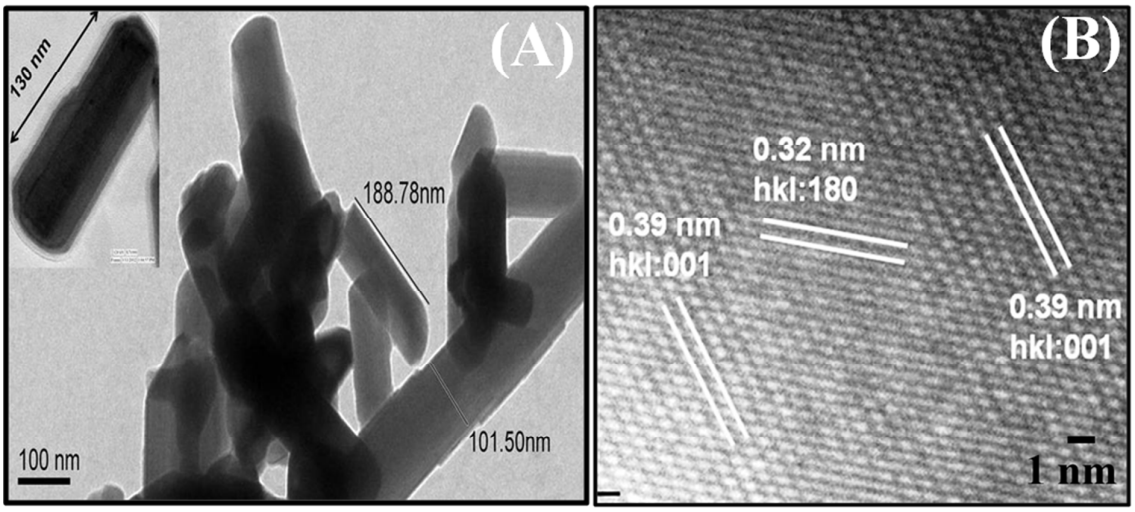

FIG.4

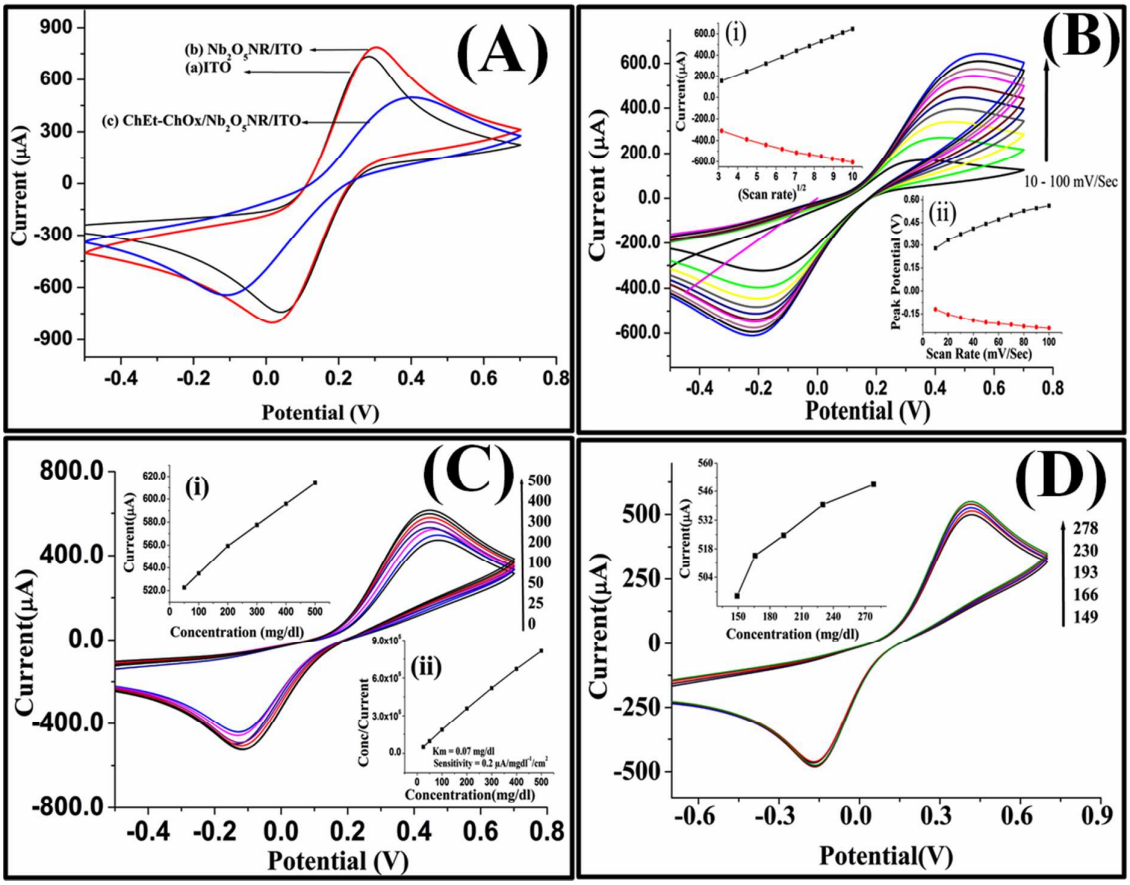

FIG.5

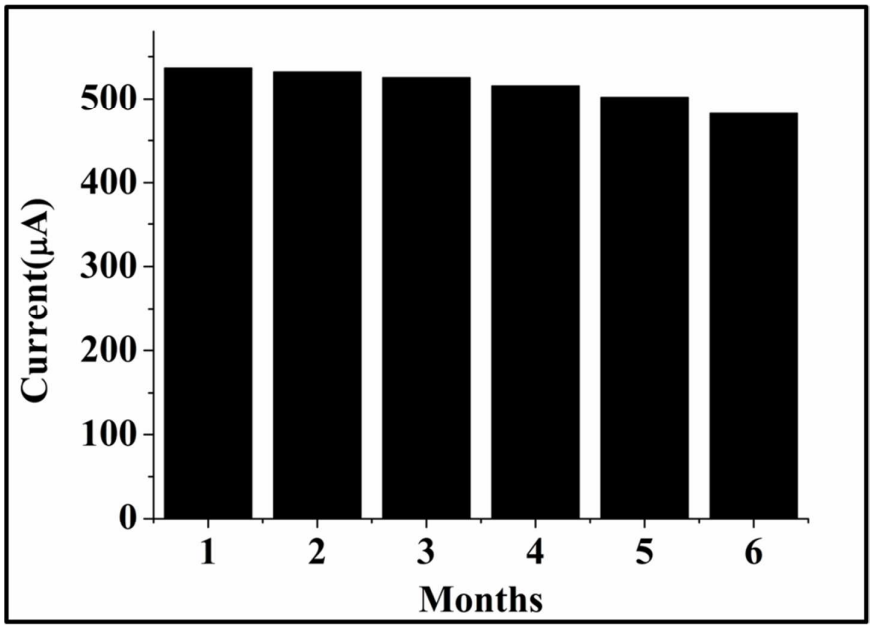

FIG.6

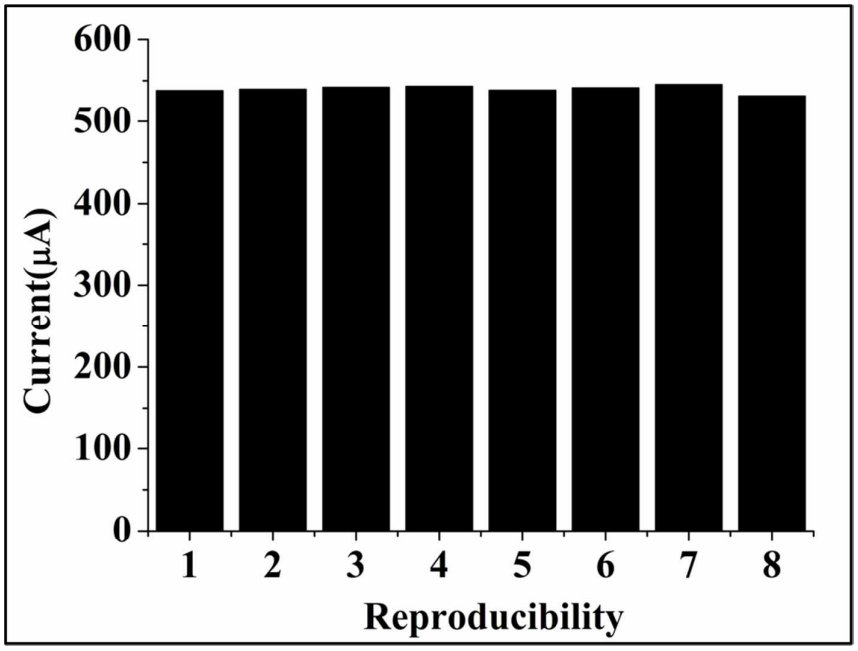

FIG.7

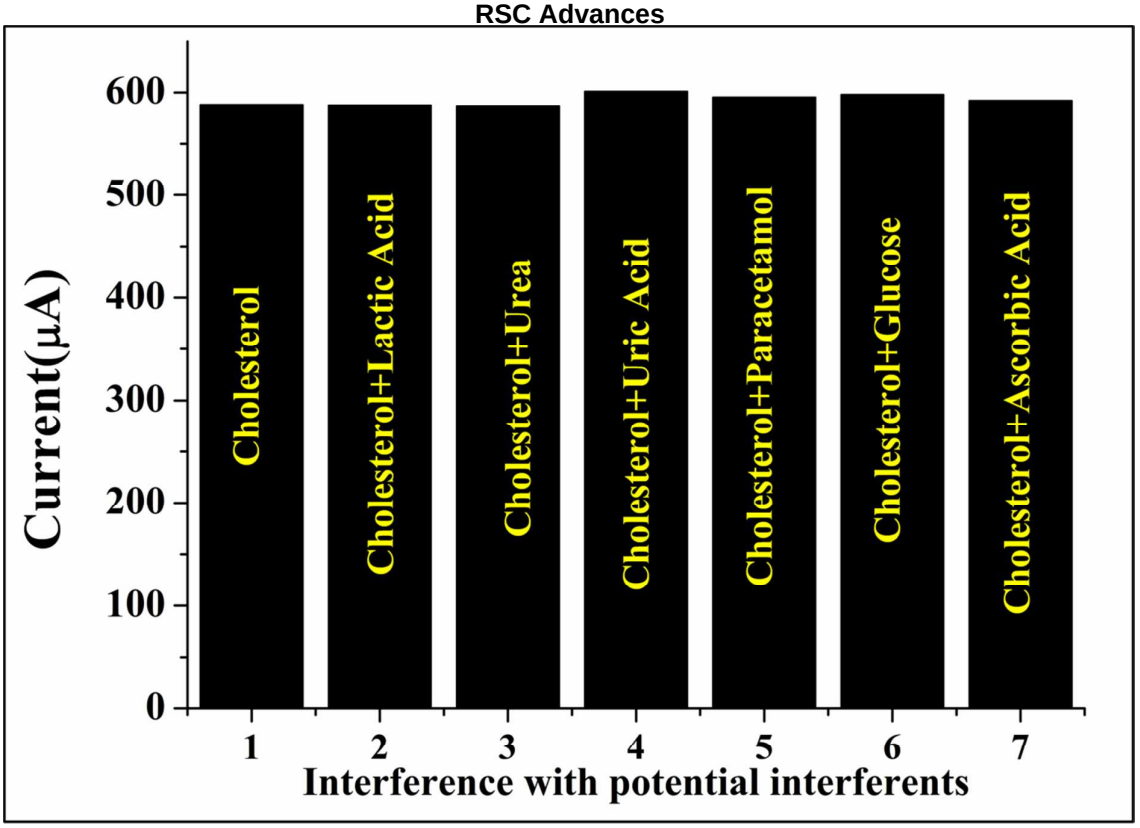

FIG.8

TABLE.1: Comparison table on performance characteristics of metal oxide based cholesterol biosensor.

Working electrode	Detection range (mg/dl)	Sensitivity ($\mu A/mgdL^{-1}cm^{-2}$)	K_m Value (mg/dl)	Cost (based on element availability)	Response time (s)	Shelf-Life (days)	Ref.
Nano CeO_2	10-400 mg/dl	$2\mu A/mgdL^{-1}cm^{-2}$	76 mg/dl	Expensive (Rare earth metal)	15sec	-	29
NanoFe_3O_4	50–200 mg/dL	-	17 mg/dL	Inexpensive	-	15 days	33
NanoZnO_2	25–400 mg/dL	-	80 mg/dL	Inexpensive	15 sec	75 days	34
Nano NiO	10 - 400 $mgdL^{-1}$	$0.808\mu A/mgdL^{-1}$ cm^{-2}	(25.52mg/dl)	Inexpensive	15 sec	70 days	35
Nano CoO	4.2 – 50 µM	0.043 µA/ µM	(18.94mg/dl)	Inexpensive	15 sec	---	36
Nano-Tm_2O_3	8–400 mg/ dl	$0.9245\mu A$ $(mg/dlcm^{-2})$	-	Expensive (Rare earth metal)	40 s	---	37
NanoNb_2O_5NR	25-500mg/dl	$0.267\mu A$ $(mg/dlcm^{2})$	0.07mg/dl	Inexpensive	< 10 Sec	>180 days	Present work